Design of Acoustic Emission Sensor Layout for Source Localization

Zhang, F.; Yang, Y.; Hendriks, M.A.N.

Publication date
2023

Document Version
Final published version

Published in
Proceeding of the 12th International Conference on Structural Health Monitoring of Intelligent Infrastructure (SHMII-12)

Citation (APA)
Zhang, F., Yang, Y., & Hendriks, M. A. N. (2023). Design of Acoustic Emission Sensor Layout for Source Localization. In *Proceeding of the 12th International Conference on Structural Health Monitoring of Intelligent Infrastructure (SHMII-12)* (pp. 462-468). International Society for Structural Health Monitoring of Intelligent Infrastructure, ISHMII.

SHMII-12: 12th International Conference on Structural Health Monitoring of Intelligent Infrastructure
October 19-22, 2023, Hangzhou, Zhejiang, China. Paper ID# SS8-ITM-P078, Zhang

Design of Acoustic Emission Sensor Layout for Source Localization

Fengqiao Zhang[1], Yuguang Yang[1], Max A.N. Hendriks[1,2]
[1]Department of Civil Engineering and Geoscience, Delft University of Technology, Delft, the Netherlands
[2]Department of Structural Engineering, Norwegian University of Science and Technology, Trondheim, Norway.
Email : f.zhang-5@tudelft.nl, yuguang.yang@tudelft.nl, m.a.n.hendriks@tudelft.nl

ABSTRACT: Acoustic emission (AE) is a favourable technique for crack detection in concrete structures. One main objective of AE is to estimate the origin of the source which is called source localization. The spatial distribution of the estimated source locations indicates the cracking location. To perform an effective source localization, a proper design of sensor layout is an important basis. An unjustified sensor layout may lead to larger localization errors or missing of AE events. Many studies in literature apply AE source localization but do not provide a rational explanation of the design of sensor layouts. This paper presents a comprehensive procedure for designing a sensor layout, including determination of measuring zone, establishment of sensor spacing and design of sensor placement. The provided method is demonstrated in an experiment that involves AE monitoring of failure of a full-scale reinforced concrete beam. We use the experiment to further study the influence of the sensor layout. The results of this paper suggest several criteria to guide the design of sensor layouts for source localization.

KEY WORDS: acoustic emission, source localization, sensor layout, localization efficiency.

- EXTENDED ABSTRACT

Acoustic emission (AE) is a favourable technique for detecting cracks in concrete structures especially internal cracking. A primary aim of AE is the estimation of the origin of a source, commonly referred to as source localization. The spatial distribution of these estimated source locations indicates the locations of the cracking.

Achieving effective source localization requires careful design of sensor layouts. An unjustified sensor layout could yield larger localization errors or missing of some AE events. Despite the widespread use of AE source localization in literature, many studies did not offer a logical explanation for their chosen sensor layout.

In response to this, our paper presents a comprehensive procedure for designing a sensor layout. This includes determining the measurement zone, establishing the appropriate sensor spacing, and designing the sensor placement. At each step, we provide a logical basis for the criteria to be considered.

To demonstrate our proposed method for designing sensor layouts, we use AE data gathered during a failure test of a full-scale reinforced concrete beam. Based on the original sensor layout, we strategically use only a portion of the sensors to study the effect of sensor spacing on source localization results. Additionally, we suggest adjustments to sensor placement to enhance efficiency in source localization.

The results suggest several criteria to guide the design of sensor layouts for source localization.

- Determination of the measuring zone: It is essential to identify a critical region to serve as the measuring zone. For full-scale structural members, it is not feasible to use AE sensors to cover the entire structure. The measuring zone depends on the structural type, failure mode, and surface condition. Structural analysis and on-site inspection are needed to decide the measuring zone.
- Establishment of the sensor spacing: It is needed to measure the wave propagation properties including the wave velocity and attenuation. The setup of the measurement is described in this paper. The aim is to find the maximum sensor spacing that allows signals from an AE event, even after wave attenuation, to be received by a sufficient number of sensors for source localization—specifically, three sensors for 2D localization and four sensors for 3D localization.
    - For monitoring flexural cracking and shear cracking, we recommend estimating the crack spacing. The sensor spacing should not exceed the crack spacing if the goal is to distinguish each crack individually. This is because when two cracks are present within a single sensor grid area, AE events from the second-opening crack may not be accurately localized.
- Design of the sensor placement: For each proposed sensor layout, it is suggested to perform an analysis of the required source amplitude distribution. The computing of the required source amplitude is described in this paper. A more efficient sensor layout should yield a lower required source amplitude, enabling more AE events to be localized. Preliminary findings suggest that a more evenly distributed sensor placement within the measuring zone with the determined sensor spacing is beneficial.

1 INTRODUCTION

Many existing concrete structures are nearing the end of their service life [1, 2]. It is crucial to make informed decisions regarding the interventions to these bridges—whether to demolish, maintain, or take no action—considering the public safety and the sustainable construction. To make informed decision, an effective monitoring of the health condition of existing concrete bridges is essential.

Cracking is a key performance indicator for reinforced concrete structures [3, 4]. It may reduce the structural capacity or accelerate other deteriorations, such as reinforcement corrosion. As a result, monitoring concrete cracking is important. Various techniques can measure concrete cracking, including linear variable differential transformers (LVDT), unmanned aerial vehicles (UAV), digital image correlation (DIC) [5]. Among these, acoustic emission (AE) stands out due to its sensitivity to cracking, its ability to detect internal damages, its real-time crack detection capabilities, and the ease of sensor installation on the bridge surface [6].

AE works on the principle that sudden changes in concrete, such as cracking, release energy and generate elastic waves. These waves propagate in the concrete from the crack to the sensor location. By processing the received signals, it is possible to estimate the origin of the source (which is called source localization) [7, 8], distinguish the source type such as cracking or friction (which is called source classification) [9, 10], and determine structural integrity [11].

AE analysis is heavily dependent on the raw data received by the sensors. To ensure reliable data acquisition, the sensor layout needs to be carefully designed. An effective layout should capture sufficient signals to detect cracks while being efficient by using the minimal number of sensors needed.

However, there is a lack of studies in the literature that rationalize AE sensor layout designs. To the authors' knowledge, most studies either employ as many sensors as feasible to gather more information, or reduce the number of sensors to increase efficiency. The design of AE sensor layout is mostly empirical, lacking clear and consistent reasoning for the chosen sensor layout. A cost-benefit evaluation of sensor layout is available, where the cost represents sensor expenses and the benefit refers to the information gained [12]. But the evaluation does not take into account the distinctive methodology of source localization. A specific approach of designing the sensor layout for source localization is needed considering the practical measurement needs, feasibility, source localization accuracy and efficiency.

This paper introduces a comprehensive approach for designing a sensor layout for source localization, which includes determining the measuring zone, establishing sensor spacing, and planning sensor placement. We demonstrate this procedure using AE data from a full-scale reinforced concrete beam failure test. The signals from flexural and shear cracks are used. By selectively using only a portion of sensors from the original sensor layout, we study the impact of sensor spacing on localization results. With the determined measuring zone and sensor spacing, we further analyse the influence of sensor placement on the source localization and propose an optimized sensor placement.

The results of this paper suggest several criteria to guide the design of sensor layouts for source localization. The proposed rationalized procedure to design a sensor layout enables more effective data collection, paving the way for meaningful data analysis and decision-making.

2 DESIGN OF SENSOR LAYOUT FOR SOURCE LOCALIZATION

2.1 Source localization

Source localization algorithms estimate the location of an AE event. The commonly used method is based on the arrival times of the signals [7]. Inputs are arrival times, sensor locations and wave speed. The basic rule is that the estimated wave propagation distance from the source to the receiver should meet with the measured wave propagation distance.

Following the basic rule, the source localization in this paper uses the grid search method [13] by searching the grid point which gives the minimum residual between estimated and measured differential wave propagation distance:

$$r_k = \sum_{i=1}^{N_\mathrm{r}-1} \sum_{j=i+1}^{N_\mathrm{r}} \left[d_{k,i} - d_{k,j} - c \cdot (t_i - t_j)\right]^2, \quad k \in \{1,2,\cdots,N_\mathrm{g}\} \tag{1}$$

where, N_g is the number of grid points that discretize the measuring zone, N_r is the number of sensors, $d_{k,i}$ is the measured distance between grid point k and sensor i, $d_{k,j}$ is the measured distance between grid point k and sensor j, c is the wave speed, t_i is the arrival time at sensor i, and t_j is the arrival time at sensor j. The location of grid point k that has the minimum r_k is the estimated source location.

2.2 Determination of measuring zones

The first step of designing a sensor layout is to determine the measuring zone. The determination of measuring zone depends on the structural type, the failure mode and the surface condition.

For reinforced concrete structures, flexural failure is a common failure mode. Flexural cracks form at the cross-section with the maximum bending moment. The width of these cracks increases with the load until the steel reinforcement at the flexural crack yields. To indicate the flexural cracking, the measuring zone should cover the region with the maximum bending moment [14, 15], especially the edge of the cross section that encompasses the largest tensile stresses.

Another concern for reinforced concrete structures is flexural shear failure. As the load increases, flexural cracks also form at the cross-section in the shear span. These cracks typically start vertically and then bend towards the loading point, resulting in what is known as a flexural shear crack. If the flexural shear crack damages the compressive strut (the compressive region between the load and the support), the structure fails suddenly and catastrophically. To indicate the flexural shear failure, according to various theoretical models [3, 16, 17], cracking in the flexural region and shear region especially the compressive strut should be monitored.

For each structural member to be monitored, structural analysis of critical region is necessary, since using AE sensors to cover the entire structure is not feasible especially for large-scale structures such as bridges of large span.

The structural surface condition also needs to be inspected when determining the measuring zone. AE sensors need

accessibility to the structural surface and require a smooth surface condition.

2.3 Establishment of sensor spacing

The next step is to determine the sensor spacing. Sensor spacing influences the source localization due to wave attenuation. The effects would be (1) large source localization error or (2) missing of AE events.

For an AE source, the signals received by the farther sensor have larger attenuation. When after attenuation, the direct P-waves could not be detected, the first arrival will be picked at a later part of the signal (which could be other wave modes, diffractions or reflections). Using these arrival times would generate larger source localization errors. To reduce this effect, the sensor spacing needs to be limited to ensure that the direct P-waves can be detected. Influence of sensor spacing on the source localization error and the resultant limitation on sensor spacing have been elaborated in our previous study [18].

The other effect, missing of an AE event, occurs when an insufficient number of sensors can receive the direct P-waves after attenuation. The required minimum number of sensors are three for 2D localization and four for 3D.

As can be seen, to determine the sensor spacing, it is vital to measure the wave propagation property especially the wave attenuation. The maximum sensor spacing needs to be adjusted according to the wave attenuation properties and the signal and the noise level. This paper provides an approach for measurement of wave propagation as below.

A number of sensors were installed in a line in the uncracked area (Figure 1a). We used 14 sensors in our measurement. The sensor spacing was 40 mm. The first transducer was used as a source and induced the source signal. The induced source was received by other sensors after propagation. The sensor closest to the source was selected as the reference sensor. The arrival time and peak amplitude of the signals received by every sensor were calculated (Figure 1b) and compared to those from the reference sensor. In this way we obtained the travel time and amplitude drop from the reference.

Figure 1c and d show the travel time and amplitude drop from the reference against the wave travel distance measured on a beam specimen. The travel time was determined by the P-waves which arrived first. By dividing the travel distance by the travel time, the wave speed was estimated to be around 4100 m/s (Figure 1c).

The amplitude drop comes from two sources: the material attenuation and the geometric spreading loss [19]:

$$f(d) = \alpha \cdot d + 20 \cdot \log_{10}\left(\frac{d}{r}\right) \quad (2)$$

where α is the material attenuation factor which is estimated to be 20 dB/m, d is the wave travel distance, and r is the source sphere radius which is taken as the radius of the sensor 0.015 m. The term α·d is the material attenuation, which is assumed the same for P-waves and surface waves, and the term 20log10(d/r) is the geometric spreading losses of P-waves, while the value is 10log10(d/r) for surface waves.

Figure 1d shows the attenuation functions fitted with the measured amplitude drop. It should be noted that the measured peak amplitude drop primarily describes the attenuation of surface waves which contains larger energy. Therefore, we used the measured amplitude drop to fit the attenuation of surface wave. In the source localization we use the attenuation of P-wave as it arrives first. Therefore, we derive the attenuation of P-waves from surface waves by assuming a same material attenuation factor α = 20 dB and a known geometric spreading loss 20log10(d/r). In the presented measurement, after 1 m, P-waves attenuate around 55 dB. This means that for source amplitude of 100 dB and threshold of 50 dB, after 1 m, P-waves cannot be detected by the sensors. The sensor spacing should be within 1 m.

The presented measurement was performed on the specimen that is introduced in Section 3. Therefore, the measured wave propagation properties are used in the following design of sensor layout.

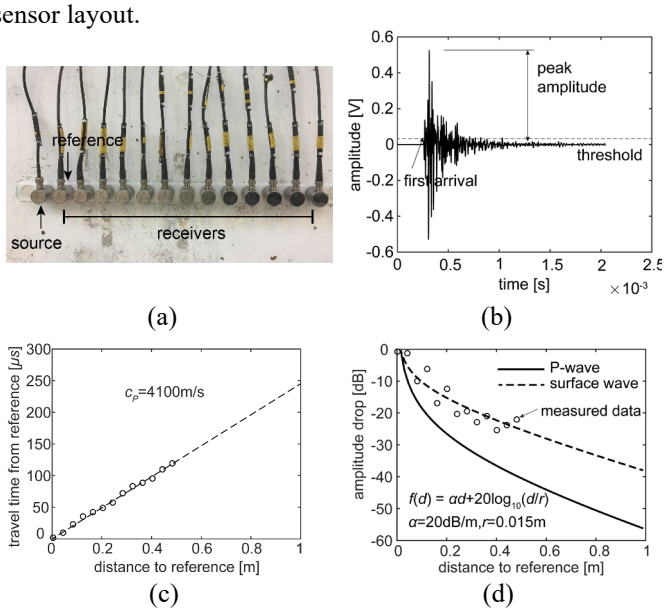

Figure 1 Preliminary test on wave propagation properties: (a) test setup, (b) signal parameters of arrival time and peak amplitude, (c) estimation of wave speed of P-wave, (d) estimation of wave attenuation of surface wave and P-wave.

2.4 Design of sensor placement

With the determined measuring zone and sensor spacing, the number of applied sensors can be estimated. But even with this information known, the sensor placement is still flexible and can influence the localization results. The influence of sensor placement is on the sensitivity to AE events at different locations in the measuring zone. The influence is explained below.

As mentioned above, a 2D source localization requires at least three sensors can receive the signal, and a 3D localization requires at least four sensors. When the third/fourth closest sensor cannot receive the signal, the farther sensors cannot receive due to more attenuation. Here we assume that the attenuation only depends on the sensor-to-source distance $f(d)$. We would then have an insufficient number of sensors to locate an AE event. Therefore, the signal amplitude received at the third/fourth closest sensor determines whether an AE event can be located in 2D/3D.

Figure 2 exemplifies a 2D sensor layout with three sensors. The threshold value at each sensor is 50 dB. Supposing that an AE event is at location p_1, the decisive sensor is the third closest sensor to the source, which is R_3 with distance of d_{13}. Considering the attenuation function f of distance d, to ensure the signal can be received by R_3 after attenuation, the source amplitude is required to be larger than $50 + f(d_{13})$. At another

location p_2, the third closest sensor is of d_{23} distance ($d_{23} < d_{13}$), the required source amplitude is $50 + f(d_{23})$, which is smaller than $50 + f(d_{13})$. This means that at location p_2, AE events of a smaller amplitude can be located. The sensor layout is more sensitive to AE events at location p_2 than p_1.

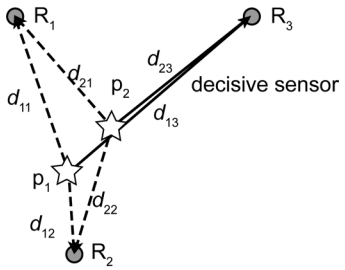

Figure 2 Illustration of the decisive sensor in 2D source localization.

We use the required source amplitude to evaluate the sensitivity of a sensor layout to AE events at a location. The required source amplitude in dB at a location p is calculated as the sensor threshold level plus the wave attenuation from the studied location to the decisive sensor:

$$A_{p,req} = A_0 + f\left(d_{p,r_d}\right) \tag{3}$$

where r_d is the decisive sensor which is the third (for 2D) or fourth (for 3D) closest sensor, $d_{p,rd}$ is the distance between the location p and the decisive sensor r_d, $f(d_{p,rd})$ is the attenuation in dB, A_0 is the threshold in dB.

Figure 3 shows the required source amplitude at every possible source location in the example. The threshold at each sensor is 50 dB and the attenuation function $f(d)$ takes the one measured in the experiment described in Section 2.3. We find a lower required source amplitude in the centre of a sensor grid than on the edge (70 dB and 81 dB respectively). This means that AE events with amplitude in range of 70-81 dB can only be located when they occur in the centre of a sensor grid. This sensor layout is more sensitive to AE events in the centre of a sensor grid.

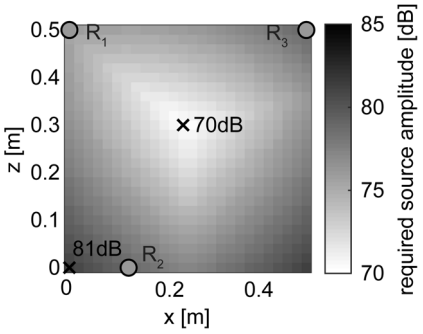

Figure 3 Distribution of the required source amplitude for localization in a sensor layout

In case one compares the number of AE events at different locations in the measuring zone, the influence of sensor placement needs to be reduced. A method is to set up a source amplitude threshold that only AE events with the source amplitude over this threshold are counted. The threshold is taken as the highest value in the distribution of required source amplitude in the measuring zone. When an AE event is localized, we first estimate its source amplitude according to the received signal amplitude and the wave attenuation after propagating from the source to the receiver. If the estimated source amplitude is over the pre-set threshold, the AE event is counted. In this way, the required source amplitude in the whole measuring zone is unified, giving a same sensitivity to AE events at different locations.

This calibration method straightforwardly eliminates AE events that have a source amplitude below a predetermined threshold. This approach inevitably leads to the removal of lower energy/amplitude AE events. The severity of the impact—specifically, the percentage of AE sources that get filtered out—depends on the distribution of the source amplitude.

3 DESCRIPTION OF THE EXPERIMENT

The proposed approach for designing sensor layout is demonstrated using the AE monitoring of failure test of a full-scale reinforced concrete beam.

The test, named as I123A, is originally designed for the purpose to study shear behaviour [20], where multiple cracks including flexural cracks and shear cracks were generated. AE signals from concrete cracking were recorded and source localization was performed to estimate the crack location. This section introduces the test setup and the sensor layout.

3.1 Test setup

The dimensions of the beam are 10000 mm × 300 mm × 1200 mm. The concrete class is C65. The reinforcement consists of 8Ø25 plain bars. Figure 4 shows the reinforcement configuration with the position of load and supports. The tested end does not have shear reinforcement.

The beam was simply supported and loaded by a single point load. The distance between the centre of the point load and the closer support (defined as shear span) was 3000 mm. The load was applied through a hydraulic jack in a displacement-controlled manner. The loading speed was 0.02 mm/s. Detailed loading history can be found in the measurement report [20].

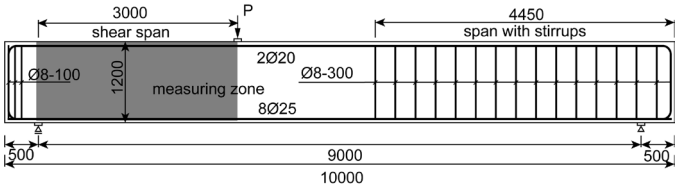

Figure 4 A sketch of beam configuration including beam dimension, reinforcement layout, locations of supports and load and measuring zone.

3.2 Sensor layout

The measurements during the tests included sensors for load measurement (load cell), displacement measurement (LVDTs, lasers, DIC), and AE measurement. This paper focuses on AE measurement, with others can be found in the measurement report [20].

Figure 5 shows the AE sensor layout with the crack pattern at failure marked. A total of 13 sensors were applied, covering a measuring zone of 2000 mm × 1112 mm in the *x*-*z* plane. The sensor spacing is mostly 500 mm, with maximum 612 mm.

The applied AE sensor is of type R6I from MISTRAS [21]. The central frequency is 60 kHz. The sensor was fixed to the specimen by a steel holder. Grease-like material from

MOLYKOTE [22] was used as couplant between the sensor surface and structural surface.

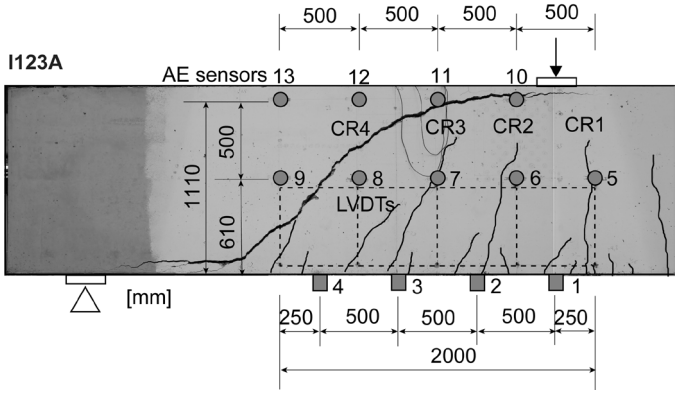

Figure 5 Locations of AE sensors, load and one support and the crack patterns.

4 INFLUENCE OF THE SENSOR LAYOUT ON SOURCE LOCALIZATION

This section first shows the localization results using the original sensor layout (Section 4.1). Then, by selectively using a portion of sensors, the effect of sensor spacing is studied (Section 4.2). Moreover, with the given measuring zone and the sensor spacing, the influence of sensor placement is studied (Section 4.3).

4.1 Source localization results using the original sensor layout

Figure 6 shows the localization results of AE events during the entire loading process (excluding those during unloading). A total of 14989 AE events were localized, indicating the opening of cracks CR1-CR4 in the measuring zone. CR1 first opened where the bending moment was the largest. With increasing load, CR2, CR3 and CR4 opened sequentially. CR4 was the critical shear crack that shortly after opening of CR4, the beam failed in shear.

The determined measuring zone is able to cover the cracking activities from flexural cracking (CR1) to shear cracking near failure (CR4), which meets the experimental need to study the shear behaviour of the specimen. Moreover, in the measuring zone, the sensor layout can capture the crack pattern clearly, even the secondary cracks in the bottom of the beam can be detected (as observed near CR3).

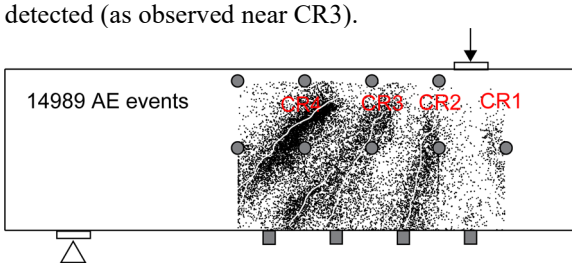

Figure 6 Source localization using all sensors 1-13, with the sensor spacing of 0.5 m.

4.2 Influence of the sensor spacing

The original sensor layout deploys a total of 13 sensors, with a spacing of 0.5 m between each sensor. We now explore the source localization performance when fewer sensors are utilized.

Firstly, we decrease the number of sensors by selecting every other sensor, specifically sensor numbers 1, 3, 5, 7, 9, 10 and 12. For each row of sensors at the same height, the sensor spacing is increased to 1 m. However, due to the staggered alignment of sensors in different rows in the x direction, the overall sensor spacing remains at 0.5 m.

Figure 7 presents the localization results when fewer sensors are used, while maintaining the same sensor spacing of 0.5 m. Despite a significant reduction in the number of localized AE events (down to 7620), the patterns of cracks CR1-CR4 can still be identified. Nevertheless, detailed patterns within the sensor grid area of sensors 3, 7, and 9 are missing, which include the secondary crack adjacent to CR3 and the bottom portion of CR4. This missing of AE events occurs when more than one crack is present within a sensor grid area. For instance, when CR4 developed, the presence of CR3 further attenuated the waves from CR4 to the sensors, particularly sensor 3, resulting in waves that could not be received. Consequently, an insufficient number of sensors could receive signals from CR4, which therefore could not be localized.

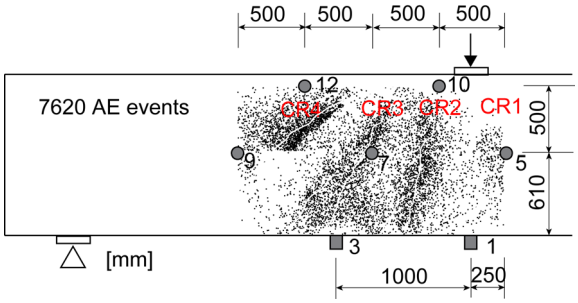

Figure 7 Source localization using sensors 1, 3, 5, 7, 9, 10 and 12, with the sensor spacing of 0.5 m.

Next, we further decrease the number of sensors by using only sensors 1, 3, 11, and 13, thereby increasing the sensor spacing to 1 m. Figure 8 displays the localization results when using a sensor layout with a spacing of 1 m. The coverage area of the sensors is reduced, but within this area, the patterns of cracks CR2, CR3, and the tip of CR4 can be clearly recognized. In the corner near sensor 3, very few AE events are localized. This is because for sources located at the corner, the distance for wave travel distance to other sensors may exceed 1 m, which causes the P-waves to be attenuated below the threshold and cannot be detected by a sufficient number of sensors for localization, as explained in Section 2.3.

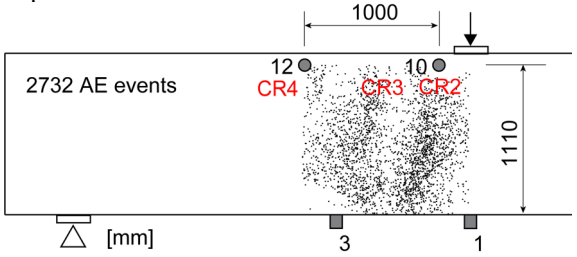

Figure 8 Source localization using sensors 1, 3, 10 and 12, with the sensor spacing of 1 m.

We increase the sensor spacing further to 1.5 m, using only sensors 1, 4, 10, and 13 to carry out source localization. Figure 9 presents the localization results using a sensor spacing

of 1.5 m. The crack pattern becomes nearly unrecognizable, with only parts of CR2 and CR4 vaguely shown. Furthermore, in the corners near the sensors, AE events are hardly localized. This is because the travel distance to other sensors exceeds 1 m, which prevents enough sensors from receiving the P-waves necessary for source localization.

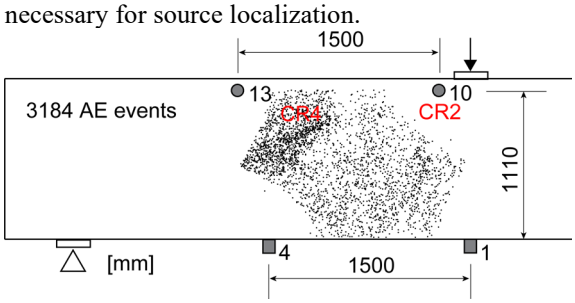

Figure 9 Source localization using sensors 1, 4, 10 and 13, with the sensor spacing of 1.5 m.

The aforementioned results imply that for clear identification of the crack pattern, the maximum sensor spacing should be 1 m, which aligns with the result from our wave attenuation measurement in Section 2.3. Additionally, the sensor spacing should be configured such that a maximum of one crack can occur between two sensors. Otherwise, the presence of an existing crack could interfere with the localization of the new cracking.

4.3 Influence of the sensor placement

As described in Section 2.4, given a sensor layout, the localization is more sensitive to sources in the centre of the sensor grid, being able to localize an AE event with lower source amplitude. For a group of AE events, if they are near the centre of a sensor grid, more events can be localized. This may interfere the identification of crack patterns which uses the spatial distribution of AE events.

Figure 10 shows the required source amplitude at every possible source location in the sensor layout of test I123A. The calculation of the required source amplitude follows the method in Section 2.4. The threshold at each sensor is 50 dB and the attenuation function take the one measured in Section 2.3.

A difference between 71 dB and 82 dB is found in the centre and edge of the sensor grid. This shows that AE events with source amplitude in the range of 71-82 dB can only be localized if the events occur in the centre of the sensor grid.

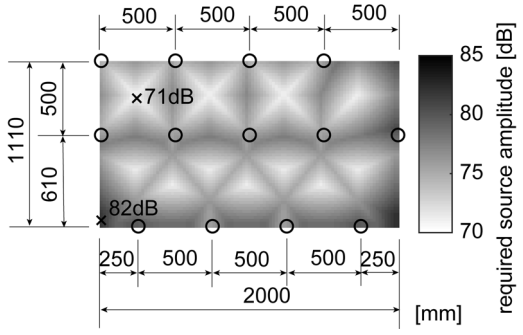

Figure 10 The required source amplitude distribution, showing different sensitivities.

To ensure an equitable count of AE events across all locations, a unified source amplitude threshold is suggested. This threshold should be set at the maximum value of the required source amplitude within the measuring zone. When an AE event is localized, its source amplitude should first be estimated based on the received signal amplitude and the wave attenuation from the source to the receiver. If the source amplitude exceeds the pre-defined threshold, the AE event is counted. This method allows AE events from different locations to be counted under the same source amplitude requirement.

However, this calibration method has the disadvantage of discarding some localized AE events that could have been useful. For instance, as shown in Figure 10, if the threshold is set at 82 dB, which is the highest value in the distribution, all AE events with amplitude lower than 82 dB will be dismissed. Therefore, an optimal sensor layout should have a lower threshold, thus excluding fewer AE events.

An improved sensor layout is displayed in Figure 11, wherein the sensors are more evenly distributed throughout the measuring zone. This adjustment leads to a reduction in the highest value to 80 dB and lowers the source amplitude threshold from 82 dB to 80 dB. As a result, more AE events are retained. While further improvements to the sensor layout might be feasible to lower the source amplitude threshold, such enhancements are not explored in this paper.

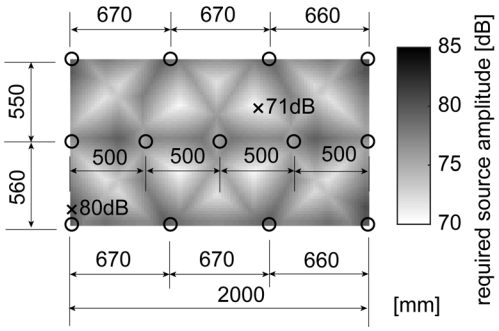

Figure 11 The required source amplitude distribution after sensor layout adjustment.

5 DISCUSSION

Several factors must be taken into account when designing a sensor layout for AE source localization. Primarily, the sensor layout should meet practical measurement requirements. Depending on the structural type, the critical failure mode, and the condition of the structural surface, the first step is to establish a measuring zone. This stage would benefit from the expert judgement of structural engineers, as well as an on-site inspection. The presented experiment suggests that, to detect shear failure in a 10-m span of a concrete bridge, a measuring zone ranging from 2-3 m is required.

Subsequently, the sensor spacing must be determined, which depends on the wave attenuation property. Measurements of wave attenuation properties are required, and a procedure for this is provided in Section 2.3. The general rule is that the P-waves should be received by at least three sensors for 2D source localization and four sensors for 3D source localization. Moreover, the sensor spacing is better to be smaller than the estimated crack spacing to ensure that only one crack occurs between two sensors.

It is interesting to note that, for flexural and shear cracks that initiate from the bottom of the structure and propagate towards the compressive zone, sensors placed on the top and bottom surfaces are sufficient. There's no need for sensors at intermediate heights. This facilitates a more flexible sensor layout design, especially considering that typically only the top and bottom surfaces are accessible.

Once the measuring zone and sensor spacing are determined, the sensor placement can also be optimized to increase the efficiency of source localization. Our findings suggest that a more evenly distributed sensor layout can minimize the variance in sensitivities to AE events within the measuring zone. Further enhancements can be made by fine-tuning the sensor placement.

Considering the varying sensitivities to AE events within the measuring zone, it is recommended to apply a source amplitude filter that only counts sources with an amplitude exceeding a certain threshold. This calibration allows for a fair comparison of the quantity of AE events at different locations, which forms an important basis for quantifying crack magnitude using the number of AE events.

6 CONCLUSTION

Designing acoustic emission (AE) sensor layout is an important step to guarantee a reliable data acquisition for the future data processing and analysis. The design of sensor layouts should consider the practical needs and applicability, the source localization accuracy and efficiency.

With the above considerations, this paper rationalizes the procedures of designing a sensor layout, from determining the measuring zone, to establishing the sensor spacing, and the designing of sensor placement. The procedure was applied in AE monitoring of shear failure of a full-scale reinforced concrete beam. We find that the within the maximum sensor spacing of 1 m, the crack patterns can be clearly identified. And the sensor placement is suggested to be more evenly distributed to perform a more efficient source localization.

For applications in other cases, measurement on wave propagation properties to decide the maximum sensor spacing is needed. And analysis of the required source amplitude distribution is needed to optimize the sensor placement.

The results of this paper suggest several criteria to guide the design of sensor layout for an efficient source localization.

ACKNOWLEDGMENTS

The authors would like to acknowledge Rijkswaterstaat (the Dutch Ministry of Transportation and Water Management) who partly supported this research.

REFERENCES

[1] E.O.L. Lantsoght, C. van der Veen, J. Walraven, A. de Boer, Recommendations for the shear assessment of reinforced concrete slab bridges from experiments, Structural Engineering International 23(4) (2013) 418-426.
[2] Rijkswaterstaat, Vervanging en Renovatie: Prognose voor de periode 2023 tot en met 2050, forecast report, the Netherlands, 2022.
[3] A. Muttoni, M. Fernández Ruiz, Shear strength of members without transverse reinforcement as function of critical shear crack width, ACI Structural Journal, 2008, pp. 163-172-163-172.
[4] Y. Yang, J. Walraven, J.d. Uijl, Shear Behavior of Reinforced Concrete Beams without Transverse Reinforcement Based on Critical Shear Displacement, Journal of Structural Engineering 143(1) (2017) 04016146.
[5] *fib*, Monitoring and safety evaluation of existing concrete structures, Elsener and Böhni2003.
[6] C. Grosse, M. Ohtsu, Acoustic emission testing: Basics for Research-Applications in Civil Engineering, 2008.
[7] T. Kundu, Acoustic source localization, Ultrasonics 54(1) (2014) 25-38.
[8] F. Zhang, Y. Yang, M. Naaktgeboren, M.A.N. Hendriks, Probability density field of acoustic emission events: Damage identification in concrete structures, Construction and Building Materials 327 (2022) 126984.
[9] M. Ohtsu, Recommendation of RILEM TC 212-ACD: Acoustic emission and related NDE techniques for crack detection and damage evaluation in concrete: Test method for classification of active cracks in concrete structures by acoustic emission, Materials and Structures 43(9) (2010) 1187-1189.
[10] F. Zhang, Y. Yang, S.A.A.M. Fennis, M.A.N. Hendriks, Developing a new acoustic emission source classification criterion for concrete structures based on signal parameters, Construction and Building Materials 318 (2022) 126163.
[11] M.U. Masayasu Ohtsu, Takahisa Okamoto, Shigenori Yuyama, Damage Assessment of Reinforced Concrete Beams Qualified by Acousitc Emission, ACI Structural Journal (2002).
[12] N. Bertola, I. Bayane, E. Brühwiler, Cost-benefit evaluation of a monitoring system for structural identification of existing bridges, 11th International Conference on Bridge Maintenance, Safety and Management, Barcelona, Spain, 2022.
[13] C. Grosse, M. Ohtsu, D.G. Aggelis, T. Shiotani, Acoustic emission testing: Basics for Research-Applications in Engineering, 2 ed., Springer Cham, Switzerland, 2021.
[14] Deutscher Ausschuss für Stahlbeton, DAtStb-Guideline: Load Tests on Concrete Structures (in German) DAfStb-Richtlinie : Belastungsversuche an Betonbauwerken, in: D.A.f. Stahlbeton (Ed.) Berlin, 2000.
[15] ACI Committee 437, Code requirenments for Load Testing of Existing Concrete Structures (ACI 437.2M-13) and Commentary, American Concrete Institute, Farmington Hills, MI, 2013.
[16] Y. Yang, J. den Uijl, J. Walraven, Critical shear displacement theory: on the way to extending the scope of shear design and assessment for members without shear reinforcement, Structural Concrete 17(5) (2016) 790-798.
[17] N.V. Tue, W. Theiler, N.D. Tung, Schubverhalten von Biegebauteilen ohne Querkraftbewehrung, Beton- und Stahlbetonbau 109(10) (2014) 666-677.
[18] F. Zhang, L. Pahlavan, Y. Yang, Evaluation of acoustic emission source localization accuracy in concrete structures, Structural Health Monitoring 19(6) (2020) 2063-2074.
[19] J.O. Owino, L.J. Jacobs, Attenuation Measurements in Cement-Based Materials Using Laser Ultrasonics, Journal of Engineering Mechanics 125(6) (1999) 637-647.
[20] Y. Yang, Shear behaviour of deep RC slab strips (beams) with low reinforcement ratio, Stevin Report, Delft University of Technology, Delft, the Netherlands, 2020.
[21] MISTRAS, R6I-AST Sensor, Product Data Sheet, MISTRAS Group Inc., Princeton Junction, NJ 08550, 2008.
[22] MOLYKOTE, MOLYKOTE 4 Electrical Insulating Compound, Product Data Sheet, DuPont de Nemours, Inc., 2018.